Published in final edited form as:
Biochem J. 2009 January 15; 417(2): 555–560. doi:10.1042/BJ20081345.

Characterisation of cytochrome bo_3 activity in a native-like surface-tethered membrane

Sophie A. Weiss[*], **Richard J. Bushby**[†], **Stephen D. Evans**[*], **Peter J. F. Henderson**[‡], and **Lars J. C. Jeuken**[‡,†,1]

[*]School of Physics and Astronomy, University of Leeds, Leeds, LS2 9JT, UK

[†]Centre for Self Organising Molecular Systems, University of Leeds, Leeds, LS2 9JT, UK

[‡]Institute of Membrane and Systems Biology, University of Leeds, Leeds, LS2 9JT, UK

Synopsis

We have developed a simple native-like surface-tethered membrane system to investigate the activity of cytochrome bo_3 (cbo_3), a terminal oxidase in *Escherichia coli*. The tethered membranes consist of *E. coli* inner membrane extracts mixed with additional *E. coli* lipids containing various amounts of the cbo_3 substrate ubiquinol-10 (UQ-10). Tethered membranes are formed by self assembly from vesicles onto gold electrodes functionalised with cholesterol derivatives. Cytochrome bo_3 activity was monitored using cyclic voltammetry with electron transfer to cbo_3 mediated by UQ-10. The apparent K_M for oxygen with this system is 1.1±0.4 μM, in good agreement with literature values for whole cell experiments and for purified cbo_3. Increasing the concentration of lipophilic UQ-10 in the membrane leads to an increase in cbo_3 activity. The activity of cbo_3 with long chain ubiquinones appears to be different to previous reports using short chain substrate analogues such as UQ-1 in that typical Michaelis Menten kinetics are not observed using UQ-10. This native-like membrane model thus provides new insights into the interaction of transmembrane enzymes with hydrophobic substrates which contrasts with studies using hydrophilic UQ analogues.

Keywords

ubiquinol oxidase; tethered bilayer; cytochrome bo_3; quinone pool

Introduction

Bacteria have extremely flexible respiratory systems which allow them to thrive in a variety of environments and growth conditions. The bacterial respiratory chain is highly branched and consists of a range of enzymes which can transfer electrons from many different substrates into a common pool of lipid soluble electron carriers, known collectively as quinones [1]. Quinones are substrates for a wide range of bioenergetic enzymes such as the photosynthetic reaction centre, the bc_1 complex and nitrate reductase. There are a number of different quinones expressed in organisms including ubiquinone or coenzyme Q, menaquinone and plastoquinone. The composition of the quinone pool in the membrane is

[1]To whom correspondence should be addressed Telephone: (+44) 0113 3433829 l.j.c.jeuken@leeds.ac.uk .

Europe PMC Funders Author Manuscripts

dependent on the species and growth conditions and ubquinone-8 is the predominant electron carrier in aerobically grown *Escherichia coli* [2].

The respiratory flexibility of prokaryotic organisms is also evident in the multiple terminal oxidases expressed by bacteria compared to the single terminal cytochrome c oxidase found in eukaryotic species. In the *E. coli* aerobic respiratory pathway there are two terminal oxidases [3] that catalyse the oxidation of ubiquinol to ubiquinone and reduce molecular oxygen to water. Cytochrome bo_3 (cbo_3) is expressed under high oxygen conditions whereas cytochrome *bd* is expressed under microaerophilic growth conditions and has a much higher affinity for oxygen [4]. Cbo_3 is structurally related to the mammalian terminal oxidase, cytochrome c oxidase [5] and its catalytic cycle is coupled to the pumping of two protons from the cytoplasm to the periplasm for every ubiquinol which is oxidised [6]. Cbo_3 contains two ubiquinol binding sites, a low affinity site (Q_L), which binds the substrate ubiquinol for catalysis and is in equilibrium with the free ubiquinone pool in the membrane, and a high affinity site (Q_H), which stabilises the semiquinone intermediate during catalysis [7]. Ubiquinol binding at the Q_L site is thought to occur in the periplasmic domain of subunit II [8] and the Q_H binding site occurs within the membrane domain of subunit I of cbo_3 [5].

The characterisation of transmembrane redox enzymes can be problematic due to the atypical nature of their substrates. Analysis of enzyme kinetics with hydrophobic substrates can be complicated by incomplete knowledge of the true substrate concentration in the membrane [9]. Long chain quinones such as UQ-10 are extremely hydrophobic and rapidly aggregate in aqueous solution, so water soluble substrate analogues such as UQ-1, UQ-2 and duroquinol are commonly used to derive kinetic and mechanistic information [10].

Appropriate membrane models are also important as it has previously been shown that some membrane bound enzymes exhibit kinetic differences compared to solubilised forms of the enzyme. The activity of cytochrome c oxidase is enhanced when solubilised with detergent. This is not due to a change in substrate availability, but is possibly related to changes in protein-protein interactions or conformational changes within the protein [11]. For cbo_3 the membrane environment has been shown to have a significant effect on the activity with UQ-1 with K_Ms ranging from 10 to 333 μM depending on the membrane composition [12, 13].

Model membrane systems are increasingly providing a suitable experimental platform to overcome these problems and study membrane peptides and proteins in their natural lipid environment [14, 15]. One such model membrane is the tethered bilayer lipid membrane (tBLM) in which a membrane is bound to a gold surface with the use of tether molecules [16, 17] that anchor the bilayer to the surface support and provide an aqueous space between the lower leaflet of the bilayer and the solid surface. These tether molecules generally contain three distinct parts, a surface reactive group which attaches to the surface substrate, a spacer group to ensure an aqueous reservoir is retained beneath the membrane and a membrane anchor. The tether molecule used in this work is EO3-cholesteryl [16, 18], which keeps the membrane close to the substrate surface. The overall quality and properties of the tethered membrane, especially in relation to its insulating properties, is dependent on many parameters including the roughness of the underlying substrate surface, grafting density of the tether molecules and their chemical composition [18, 19].

Electrochemical methods are used to investigate activity of redox enzymes using techniques such as protein film voltammetry [20]. The current produced by the oxidation or reduction of substrate is a direct measure of the turnover rate of the enzyme. The oxidation or reduction currents which are observed represent the flow of electrons from the electrode to

the enzyme possibly via a mediator. The limiting current at high overpotential increases with increasing substrate concentration in an analogous manner to the reaction velocity that is measured in solution studies and analysed in terms of Michaelis-Menten kinetics [20].

We have previously described tethered membranes that included purified c*bo*$_3$ [21]. Here, we incorporate native *E. coli* inner membranes directly into tethered membranes using a recently developed methodology in which the inner membranes are mixed with lipid vesicles [22]. In this paper we describe the formation of these native-like tethered membranes to characterise the activity of c*bo*$_3$ with native-like substrates. This method offers several advantages over more traditional methods used to characterise transmembrane bioenergetic proteins. The amount of the highly hydrophobic quinone content in the bilayer can be varied while directly monitoring the activity of the enzyme. The enzyme has been retained in its native environment and not exposed to detergents or other possible denaturing chemicals that may have an adverse effect on the protein structure or activity.

Materials and Methods

Materials

EO3-cholesteryl was made as previously described [16]. 6-Mercaptohexanol (Fluka) was used without further purification. All solvents were HPLC grade (Fisher) and used as received. Ubiquinone-10 (Sigma) was made up as 1mg/ml stock solution in chloroform and stored at −20° C. *E. coli* polar extract (Avanti) was stored in 5 mg dry aliquots stored under nitrogen at −20° C. 20 mM MOPS buffer with 30 mM Na_2SO_4 adjusted to pH 7.4 was used for the preparation of membrane extracts and all electrochemistry experiments.

E. coli inner membrane purification

E. coli inner membranes were prepared from strain GO105/pJRhisA in which the c*bo*$_3$ protein is overexpressed and no cytochrome *bd* is present [23]. *E. coli* was grown to mid-log phase at 37° C with shaking in LB medium supplemented with 500 μM $CuSO_4$ and 100 μg/ml carbenicillin. *E. coli* cells were harvested from the growth medium by centrifugation at 12000 g for 30 minutes and cell paste was frozen at −20° C overnight. Thawed *E. coli* cell paste was resuspended in MOPS/Na_2SO_4 buffer at approximately 30 mL buffer per 10 g cell paste and passed through a cell disrupter or French pressure cell at 25000 psi. Cell debris was removed by centrifugation at 12000 g for 30 minutes. The supernatant containing the membrane fraction was centrifuged at 131000 g for 2 hours and the membrane pellet was resuspended in 25% w/w sucrose-MOPS/Na_2SO_4 buffer. A 30% w/w to 55% w/w sucrose gradient with centrifugation at 131000 g for 16 hours with no deceleration or breaking was used to separate the inner membrane from the outer membrane [24]. The inner membrane fraction was removed from the sucrose gradient and washed several times with buffer and centrifugation at 131000 g for 2 hours. The protein concentration of the inner membrane preparation was determined using the Schaffner-Weissman assay [25]. Inner membrane vesicles were resuspended in buffer and stored in 5 mg/ml protein aliquots at −80° C.

Mixed Vesicle Preparation

Ubiquinol-10 solution was added to *E. coli* polar extract lipids at the desired ratio and dried under nitrogen to form a multilammelar film on the sides of a glass vial. The lipid/UQ-10 film was resuspended in buffer with vortexing and vesicles were formed by sonicating the solution to clarity for 30 minutes at 4° C. To make mixed vesicles the total weight of the inner membranes (lipid and protein) were estimated to be two times the protein weight. Inner membrane fractions were mixed with the lipid/UQ-10 vesicles at different weight ratios and sonicated for a further 30 minutes. The sonicated mixed membrane sample was centrifuged at 14500 g for 30 seconds to remove any titanium particles from the sonicator

tip. For preparation of samples by extrusion, lipid/UQ-10 mixture was passed 11 times through a 100 nm nucleopore track etched membrane, mixed with inner membrane extract and freeze-thawed three times before passing through the membrane another 11 times.

Electrodes and tethered membrane formation

Template-stripped gold (TSG) surfaces were formed as previously described [26]. Briefly, 150 nm of gold was evaporated onto a clean, polished silicon wafer. 12 mm by 12 mm clean glass microscope slides were glued to the gold surface using Epo-tek 377 and cured for 2 hours at 120° C. Once cooled the glass slides could be removed from the silicon wafer to expose the template-stripped gold surface ready for the formation of the self-assembled monolayer (SAM).

SAMs were formed by incubating a freshly exposed TSG slide in 0.11 mM EO3-cholesteryl and 0.89 mM 6-mercaptohexanol in propanol for 16 hours. This forms a 60%/40% EO3-cholesteryl/6-mercaptohexanol area ratio on the surface which was checked with impedance spectroscopy before each experiment as described by Jeuken et al [18]. The slides were rinsed with propanol and methanol and dried under nitrogen before being incorporated into the electrochemical cell.

To form mixed tethered membranes mixed membrane vesicles were added to the SAM surface at a final concentration of 0.5 mg/ml in the presence of 10 mM $CaCl_2$ and incubated for 2 hours. The surface was then rinsed several times with buffer and 1 mM EDTA to remove any traces of calcium ions in the cell.

Electrochemistry

Electrochemical measurements were carried out in a glass electrochemical cell which holds 2 mL of buffer and was thermostatted at 20° C. A saturated calomel electrode (SCE) or saturated Ag/AgCl reference electrode was used as the reference electrode (Radiometer Analytical) and a platinum wire was used as the counter electrode. All potentials in this manuscript are given versus the standard hydrogen electrode (SHE). The gold-SAM working electrode was secured at the open base of the electrochemical cell with rubber o-rings and PTFE electrode holder. The electrochemical cell was housed in a Faraday cage to minimise electrical noise and argon was used to purge the cell of oxygen. For the oxygen-activity measurements the experimental apparatus was stored and assembled inside a nitrogen filled glovebox (MBraun MB 150 B-G) where the O_2 levels were <1 ppm. No oxygen leakage from the electrochemical cell was observed during the course of the experiment. A 5 × 10 mm cross shape magnetic stirrer bar was added to the cell and the electrochemical cell was placed on a magnetic stirrer plate. This was to ensure adequate mixing of the air equilibrated buffer within the cell, especially at the working electrode region. The cell assembly with stirrer bar is shown in Figure 1. Electrochemical measurements were recorded using an Autolab (Ecochemie) electrochemical analyser with a PGSTAT30 potentiostat and a FRA2 frequency analyser. All cyclic voltammetry experiments were carried out by holding the potential at 0.444 V for 5 seconds and cycling to −0.356 V and back at a scan rate of 0.01 V/s. The UQ-10 coverage was determined at the end of each experiment by adding 1 mM NaCN to the electrochemical cell, to inhibit *cbo*$_3$, and taking a cyclic voltammogram. The area under the reduction peak gives the amount of charge required to reduce all the UQ-10 within the mixed membrane and thus the UQ-10 coverage can be calculated.

Results

Formation of tethered mixed membrane bilayers

Electrochemical impedance spectroscopy (EIS) was used to characterise the formation of tethered membranes at template-stripped gold (TSG) electrodes coated with a SAM of 60/40 (±10%) EO3-cholesteryl/6-mercaptohexanol after addition of mixed vesicles consisting of *E. coli* inner membranes mixed with phospholipids and UQ-10. EIS is very sensitive to dielectric and structural changes at surfaces and has been widely used to characterise lipid structures on electrode surfaces [18, 27]. To characterise the formation of a planar membrane the double layer capacitance was estimated from the Cole-Cole plots using the diameter of the capacitative semi-circle as shown in Figure 2a. The formation of pure phospholipid membranes on the EO3-cholesteryl system has been well characterised with a typical double layer capacitance of 0.7±0.1 μF/cm^2 for *E. coli* polar extract [18, 21]. Figure 2b shows that mixing in of even relatively small proportion of *E. coli* inner membranes already leads to an increase in the double layer capacitance. For surfaces formed with 5 to 60% (by weight) inner membranes, we find a double layer capacitance of 1.20±0.16 μF cm^{-2}. With higher amounts of inner membrane the capacitance increases and becomes irregular, which suggests that the surface is increasingly covered with vesicles. This change from bilayer to adsorbed vesicles as a function of the inner membrane particle concentration is in agreement with similar work carried out by us in which mixed supported membranes on silica were characterised using QCM-D, FRAP and AFM [22].

We note that surfaces formed with mixed membrane vesicles that were prepared with different techniques did not significantly alter the results. Inner membrane vesicles formed using a French pressure cell disruption method appeared to be smaller, more regularly shaped and intact as observed by TEM (images not shown) compared to inner membrane vesicles formed using a cell disruptor. However, this did not influence the double layer capacitance. Increasing the concentration of UQ-10 (up to 3% by weight) had no effect either. Mixed vesicles were formed using two different techniques, either extrusion after freeze/thawing or by tip sonication. Both techniques resulted in similar bilayer formation and c*bo*$_3$ activities. From these experiments it was decided to continue and carry out the enzyme activity experiments with a 17% fraction of *E. coli* inner membrane formed using the cell disruptor and with the mixed vesicles formed by tip sonication. 17% *E. coli* was used as this concentration gave the most reproducible surfaces and activity in the cyclic voltammetry experiments.

Enzyme kinetics: oxygen affinity

The activity of c*bo*$_3$ in the native membrane could be readily measured using cyclic voltammetry. The co-substrate of c*bo*$_3$ is UQ-8 (or UQ-10), which is electroactive and acts as a mediator between the electrode surface and c*bo*$_3$. The electrochemistry of quinones has been extensively studied using membrane models [26, 28]. The catalytic current in cyclic voltammetry is a measure of the coupling between the enzyme oxidation and the electrochemical reduction rate of the quinone pool [29]. At high overpotentials the electrochemical reduction rate is fast and the current directly reports on the turnover activity of the enzyme. We used 8-10 pmol/cm^2 UQ-10 in the tethered membranes to measure the kinetics as a function of oxygen concentration, because this UQ-10 content gives the maximum activity (see below).

The solution within the cell was stirred to minimise possible diffusion effects of oxygen. As seen in Figure 3a, stirring has a significant effect at low oxygen concentrations and stirring the solution in the glovebox environment with < 1 ppm oxygen already produces a detectable catalytic signal. However, at higher oxygen concentrations the stirring effect

becomes less significant and we have found no significant effect on the determined apparent K_M. The apparent K_M of *cbo*$_3$ for oxygen was determined by adding air equilibrated buffer into the anaerobic electrochemical cell and taking a single CV (Figure 3a). Under anaerobic conditions the cyclic voltammogram is the same as a control voltammogram for a phospholipid tethered membrane containing UQ-10 [26]. At low oxygen concentrations some catalytic activity is observed but the UQ-10 reduction signal still appears as a peak and the reverse trace is clearly different from that of the forward trace. As the concentration of oxygen within the electrochemical cell is increased the catalytic reduction signal increases and the voltammogram changes from a peak-shape to an approximate sigmoidal wave, in which the forward and reverse scans overlay. At the highest substrate concentration the voltammogram exhibits a characteristic polarogram-like shape and the reverse trace is almost superimposible on the forward trace.

The current at −0.156 mV on the reverse scan (from low to high potential) was taken and plotted versus the overall oxygen concentration within the cell (Figure 3b). We have determined the apparent K_M for c*bo*$_3$ with oxygen to be 1.1±0.4 μM, which is within the range of previously published values [30-33].

Enzyme kinetics: UQ-10 affinity

An important aspect of this work was to develop a model membrane which can incorporate transmembrane redox proteins in their fully functioning native state and allow assays with native substrates to be carried out. Typically, activity measurements using naturally occurring quinone substrates have been problematic due to the insolubility of long-chain quinones in water, leading to the use of short-tail homologues such as duroquinol [34] and decylubiquinone [35]. The mixed membrane vesicles are made by mixing inner membranes with lipid vesicles. The latter can be made with varying amounts of ubiquinol since UQ-10 can be added to lipids before preparing the vesicles (see Materials and Methods). Here, we have formed multiple planar membranes using equal amounts of inner membranes (17% w/w) each time, but varying the amount of UQ-10. Importantly, the amount of UQ-10 within each individual bilayer could be accurately determined at the end of each experiment by the addition of 1 mM NaCN which completely inhibits c*bo*$_3$ activity.

To determine the effect of variations of UQ-10 concentration on c*bo*$_3$ activity the current at −0.156 V on the forward scan for the maximum activity was taken and plotted against the UQ-10 concentration as shown in Figure 4. The maximum activity is taken from a CV measured at ambient oxygen conditions. The large spread in the data is due to each point being derived from a separate experiment and tethered membrane. The data suggests cooperative behaviour (see dotted line in Figure 4), consistent with the fact that c*bo*$_3$ contains two distinct quinone binding sites [7]. Although the spread in the data and complex behaviour excludes an unambiguous interpretation, this technique still provides important information about the activity of c*bo*$_3$ with quinone in the native environment. As can be seen in Figure 4 a maximum activity of c*bo*$_3$ is observed with UQ-10 around 6 to 8 pmol/cm^2. Using the maximum activity of 0.6 μA and assuming that the tBLM is 5 nm thick (about 0.6 ng/cm^2), the turnover number is 4 μmol/min/mg total protein in the membrane extract. This is in good agreement to previously published values using isolated cell membranes of a similar *E. coli* strain [36].

The lowest quinone concentration determined in the mixed bilayer was measured as ~2 pmol/cm^2 at which point no UQ-10 was added and all quinone is native UQ-8 already present in the *E. coli* membrane and lipid extracts. This coverage is probably representative of native membranes and agrees with the concentration determined for tethered bilayers formed from *E. coli* polar extract only [21]. The UQ-10 concentration at the maximum activity for c*bo*$_3$ (6 to 8 pmol/cm^2) is much higher than the native concentration and also

higher than the K_M determined for the peripheral membrane protein pyruvate oxidase which has a K_M of 2 pmol/cm^2 [29]. It is also interesting to note that at even higher concentrations of UQ the activity of c*bo*$_3$ seems to decrease again, although the spread in the data makes this an ambiguous observation. This type of inhibition of quinol oxidases with UQ homologues and analogues has previously been reported in the literature [10, 37].

Discussion

We have shown that the activity of a particular transmembrane electron transfer enzyme, cytochrome *bo*$_3$, can be characterised using electrochemical methods in a near native model membrane environment. To our knowledge, there are only a few other reports that use whole cell membrane extracts to form tethered membranes [22, 38-40]. There may be a number of reasons why the double layer capacitance of the membrane increases when inner membrane particles are incorporated into the tethered bilayer. On average, proteins have a higher dielectric than lipids and this will result in some increase in the double layer capacitance of the membrane. Alternatively, a large decrease in resistance of small regions in the tethered membrane could have an impedance response that looks like an overall increase in capacitance. The breakdown of planar membrane formation at high inner membrane concentrations is probably due to the high proportion of protein in the sample inhibiting direct contact between the electrode surface and the vesicle lipids.

The tethered membrane has a mobile pool of ubiquinol, similar to that of a native membrane. Importantly, only a single homogenous UQ-10 population is observed with cyclic voltammetry indicating that the two vesicle species used to form the planar bilayer, the inner membrane particles and the *E. coli* lipids form a single continuous mixed layer across the electrode surface. The UQ concentration can be varied for each tethered membrane formed enabling studies with a physiological UQ with long hydrophobic tails rather than water soluble short chain UQ analogues.

A broad range of K_Ms (10 – 625 μM) for c*bo*$_3$ with the hydrophilic substrate analogue UQ-1 [5, 7, 10, 12, 13, 33, 35, 41] have been reported, illustrating the problems that can arise from using non-native analogues for activity studies. This diversity in K_M comes from a number of different experimental conditions that are used to assay activity. Short-chain UQ analogues have also been shown to have an inhibitory effect on enzyme activity for c*bo*$_3$ [35] and other quinol binding enzymes including complex I [35], NADH oxidase [42] and cytochrome *bd* [37], although the mechanism of inhibition is still not fully understood. As each data point in Figure 4 is obtained from a different experiment there is a broad spread in the data which seems characteristic for activity studies using long chain quinones [43, 44] adding to the difficulty in determining an accurate K_M.

We believe that some of the differences observed between c*bo*$_3$ activity with the UQ-10 used in this work and previous reports using UQ-1 may be due to localisation of different length quinones in phospholipid bilayers. Very hydrophobic quinones such as UQ-10 are known to lie parallel to the membrane plane in a homogeneous dispersion whereas shorter quinones such as UQ-1 are known to self organise more readily in highly concentrated regions with the benzoquinone ring located close to the phospholipid headgroups and with the short isoprenoid chain parallel to the phospholipid acyl chains [45, 46]. This is relevant as the Q_L site in c*bo*$_3$ is predicted to be in the extrinsic domain of subunit II [47] and thus closer to the phospholipid headgroups than the midplane of the bilayer. UQ-1 may actually give artificially enhanced reaction rates compared to native hydrophobic quinones. We suggest that the observed sigmoidal effect shown in figure 4 is likely to be due to the difference between using hydrophobic quinone substrates (our data) compared to previous kinetic studies on c*bo*$_3$ which have utilised water soluble quinones. We note that the data

points with the lowest quinone concentrations in the bilayer (Figure 4) were measured without added UQ-10 and only contained endogenous UQ-8. It cannot be excluded that this is responsible for the observed effect, although we do not believe this likely as both quinones are highly hydrophobic and located at the same positions within the bilayer. Furthermore, no differences in voltammograms were observed between bilayers containing UQ-8 and ones with additional UQ-10. Sigmoidal effects have also been reported in kinetic studies of other quinone binding enzymes from *E. coli* such as nitrate reductase [48] and cytochrome *bd*.[37]

The development of a model membrane in which all the substrates and proteins are retained and the quinones diffuse freely within a membrane is significant. When an enzyme is linked to a membrane the access and exit of quinones from the active site are necessarily restricted. The reduction from three to two dimensions for a membrane bound enzyme may have a number of important physiological consequences. These include imposing vectoriality, specific cellular location and formation of supramolecular complexes. The reduction in dimensionality may also help facilitate collisional interactions for electron transfer chains and the diffusion of hydrophobic substrates to active sites within the membrane soluble part of the enzyme.

We have demonstrated that it is possible to form a biologically relevant native-like tethered-membrane electrode surface in which the protein of interest can be assayed electrochemically. All membrane bound components are fully retained and mobile within the original native membrane and can be assayed with native substrates.

Acknowledgments

E .coli strain GO105/pJRhisA was kindly provided by Dr. R. B. Gennis (Univ. Illinois). We also thank Moazur Rahman for help with using the cell disruptor and Stefanie Jourdan for help with the French pressure cell. The production of membranes was assisted by equipment funded by the Welcome Trust and technical help funded by the European membrane consortium (EMeP). Finally, this work was funded by a BBSRC grant.

References

1. Unden G, Bongaerts J. Alternative respiratory pathways of *Escherichia coli*: Energetics and transcriptional regulation in response to electron acceptors. Biochim. Biophys. Acta-Bioenerg. 1997; 1320:217–234.
2. Collins MD, Jones D. Distribution of isoprenoid quinone structural types in bacteria and their taxonomic implications. Microbiol. Rev. 1981; 45:316–354. [PubMed: 7022156]
3. Garciahorsman JA, Barquera B, Rumbley J, Ma JX, Gennis RB. The superfamily of heme-copper respiratory oxidases. J. Bacteriol. 1994; 176:5587–5600.
4. Anraku Y, Gennis RB. The aerobic respiratory chain of *Escherichia coli*. Trends Biochem.Sci. 1987; 12:262–266.
5. Abramson J, Riistama S, Larsson G, Jasaitis A, Svensson-Ek M, Laakkonen L, Puustinen A, Iwata S, Wikstrom M. The structure of the ubiquinol oxidase from *Escherichia coli* and its ubiquinone binding site. Nat. Struct. Biol. 2000; 7:910–917. [PubMed: 11017202]
6. Puustinen A, Finel M, Haltia T, Gennis RB, Wikstrom M. Properties of the 2 terminal oxidases of *Escherichia coli*. Biochemistry. 1991; 30:3936–3942. [PubMed: 1850294]
7. Satowatanabe M, Mogi T, Ogura T, Kitagawa T, Miyoshi H, Iwamura H, Anraku Y. Identification of a novel quinone-binding site in the cytochrome *bo* complex from *Escherichia coli*. J. Biol. Chem. 1994; 269:28908–28912.
8. Satowatanabe M, Mogi T, Miyoshi H, Iwamura H, Matsushita K, Adachi O, Anraku Y. Structure-function studies on the ubiquinol oxidation site of the cytochrome *bo* complex from *Escherichia coli* using p-benzoquinones and substituted phenols. J. Biol. Chem. 1994; 269:28899–28907.

9. Fato R, Castelluccio C, Palmer G, Lenaz G. A simple method for the determination of the kinetic constants of membrane enzymes utilizing hydrophobic substrates - Ubiquinol cytochrome *c* reductase. Biochim. Biophys. Acta. 1988; 932:216–222. [PubMed: 2829962]
10. Sakamoto K, Miyoshi H, Takegami K, Mogi T, Anraku Y, Iwamura H. Probing substrate binding site of the *Escherichia coli* quinol oxidases using synthetic ubiquinol analogues. J. Biol. Chem. 1996; 271:29897–29902. [PubMed: 8939932]
11. Thompson DA, Suarez-Villafane M, Ferguson-Miller S. The active form of cytochrome *c* oxidase - Effects of detergent, the intact membrane, and radiation inactivation. Biophys. J. 1982; 37:285–293. [PubMed: 6275925]
12. Kita K, Konishi K, Anraku Y. Terminal oxidases of *Escherichia coli* aerobic respiratory chain. 1. Purification and properties of cytochrome $b_{562}o$ complex from cells in the early exponential phase of aerobic growth. J. Biol. Chem. 1984; 259:3368–3374. [PubMed: 6365921]
13. Matsushita K, Patel L, Kaback HR. Purification and teconstitution of the cytochrome-*o* type oxidase from *Escherichia coli*. Methods Enzymol. 1986; 126:113–122. [PubMed: 2856117]
14. Rossi C, Chopineau J. Biomimetic tethered lipid membranes designed for membrane-protein interaction studies. Eur. Biophys. J. Biophys. Lett. 2007; 36:955–965.
15. Chan YHM, Boxer SG. Model membrane systems and their applications. Curr. Opin. Chem. Biol. 2007; 11:581–587. [PubMed: 17976391]
16. Boden N, Bushby RJ, Clarkson S, Evans SD, Knowles PF, Marsh A. The design and synthesis of simple molecular tethers for binding biomembranes to a gold surface. Tetrahedron. 1997; 53:10939–10952.
17. Schiller SM, Naumann R, Lovejoy K, Kunz H, Knoll W. Archaea analogue thiolipids for tethered bilayer lipid membranes on ultrasmooth gold surfaces. Angew. Chem.-Int. Edit. 2003; 42:208–211.
18. Jeuken LJC, Daskalakis NN, Han XJ, Sheikh K, Erbe A, Bushby RJ, Evans SD. Phase separation in mixed self-assembled monolayers and its effect on biomimetic membranes. Sens. Actuator B-Chem. 2007; 124:501–509.
19. Koper I. Insulating tethered bilayer lipid membranes to study membrane proteins. Mol. Biosyst. 2007; 3:651–657. [PubMed: 17882328]
20. Armstrong FA. Recent developments in dynamic electrochemical studies of adsorbed enzymes and their active sites. Curr. Opin. Chem. Biol. 2005; 9:110–117. [PubMed: 15811794]
21. Jeuken LJC, Connell SD, Henderson PJF, Gennis RB, Evans SD, Bushby RJ. Redox enzymes in tethered membranes. J. Am. Chem. Soc. 2006; 128:1711–1716. [PubMed: 16448146]
22. Dodd CE, Johnson BRG, Jeuken LJC, Bugg TDH, Bushby RJ, Evans SD. Native *E. coli* inner membrane incorporation in solid supported lipid bilayer membranes. Biointerphases. 2008; 3:FA59–FA67. [PubMed: 20408670]
23. Rumbley JN, Nickels EF, Gennis RB. One-step purification of histidine-tagged cytochrome bo_3 from *Escherichia coli* and demonstration that associated quinone is not required for the structural integrity of the oxidase. Biochim. Biophys. Acta-Protein Struct. Molec. Enzym. 1997; 1340:131–142.
24. Schnaitm, Ca. Protein composition of cell wall and cytoplasmic membrane of *Escherichia coli*. J. Bacteriol. 1970; 104:890.
25. Schaffner W, Weissman C. Rapid, sensitive, and specific method for determination of protein in dilute solution. Anal. Biochem. 1973; 56:502–514.
26. Jeuken LJC, Bushby RJ, Evans SD. Proton transport into a tethered bilayer lipid membrane. Electrochem. Commun. 2007; 9:610–614.
27. Lindholm Sethson B. Electrochemistry at ultrathin organic films at planar gold electrodes. Langmuir. 1996; 12:3305–3314.
28. Marchal D, Boireau W, Laval JM, Moiroux J, Bourdillon C. Electrochemical measurement of lateral diffusion coefficients of ubiquinones and plastoquinones of various isoprenoid chain lengths incorporated in model bilayers. Biophys. J. 1998; 74:1937–1948. [PubMed: 9545054]
29. Marchal D, Pantigny J, Laval JM, Moiroux J, Bourdillon C. Rate constants in two dimensions of electron transfer between pyruvate oxidase, a membrane enzyme, and ubiquinone (coenzyme

Q(8)), its water-insoluble electron carrier. Biochemistry. 2001; 40:1248–1256. [PubMed: 11170450]

30. D'mello R, Hill S, Poole RK. The oxygen affinity of cytochrome *bo*' in *Escherichia coli* determined by the deoxygenation of oxyleghemoglobin and oxymyoglobin - K_m values for oxygen are in the submicromolar range. J. Bacteriol. 1995; 177:867–870. [PubMed: 7836332]
31. Verkhovsky MI, Morgan JE, Puustinen A, Wikstrom M. Kinetic trapping of oxygen in cell respiration. Nature. 1996; 380:268–270.
32. Rice CW, Hempfling WP. Oxygen limited continuous culture and respiratory energy - Conservation in *Escherichia coli*. J. Bacteriol. 1978; 134:115–124. [PubMed: 25879]
33. Kita K, Konishi K, Anraku Y. Purification and properties of 2 terminal oxidase complexes of *Escherichia coli* aerobic respiratory chain. Methods Enzymol. 1986; 126:94–113. [PubMed: 2856144]
34. Moody AJ, Mitchell R, Jeal AE, Rich PR. Comparison of the ligand-binding properties of native and copper-less cytochromes *bo* from *Escherichia coli*. Biochem. J. 1997; 324:743–752. [PubMed: 9210397]
35. Sakamoto K, Miyoshi H, Ohshima M, Kuwabara K, Kano K, Akagi T, Mogi T, Iwamura H. Role of the isoprenyl tail of ubiquinone in reaction with respiratory enzymes: Studies with bovine heart mitochondrial complex I and *Escherichia coli bo*-type ubiquinol oxidase. Biochemistry. 1998; 37:15106–15113. [PubMed: 9790673]
36. Minghetti KC, Goswitz VC, Gabriel NE, Hill JJ, Barassi CA, Georgiou CD, Chan SI, Gennis RB. Modified, large-scale purification of the cytochrome *o* complex (*bo*-type oxidase) of *Escherichia coli* yields a 2 heme one copper terminal oxidase with high specific activity. Biochemistry. 1992; 31:6917–6924. [PubMed: 1322173]
37. Matsumoto Y, Muneyuki E, Fujita D, Sakamoto K, Miyoshi H, Yoshida M, Mogi T. Kinetic mechanism of quinol oxidation by cytochrome *bd* studied with ubiquinone-2 analogs. J. Biochem. 2006; 139:779–788. [PubMed: 16672279]
38. Jeuken LJC, Connell SD, Nurnabi M, O'Reilly J, Henderson PJF, Evans SD, Bushby RJ. Direct electrochemical interaction between a modified gold electrode and a bacterial membrane extract. Langmuir. 2005; 21:1481–1488. [PubMed: 15697298]
39. Elie-Caille C, Fliniaux O, Pantigny J, Maziere JC, Bourdillon C. Self-assembly of solid-supported membranes using a triggered fusion of phospholipid-enriched proteoliposomes prepared from the inner mitochondrial membrane. Langmuir. 2005; 21:4661–4668. [PubMed: 16032886]
40. Jadhav SR, Sui D, Garavito RM, Worden RM. Fabrication of highly insulating tethered bilayer lipid membrane using yeast cell membrane fractions for measuring ion channel activity. J. Colloid Interface Sci. 2008; 322:465–472. [PubMed: 18387623]
41. Sato-Watanabe M, Mogi T, Sakamoto K, Miyoshi H, Anraku Y. Isolation and characterizations of quinone analogue-resistant mutants of *bo*-type ubiquinol oxidase from *Escherichia coli*. Biochemistry. 1998; 37:12744–12752. [PubMed: 9737851]
42. Landi L, Pasquali P, Cabrini L, Sechi AM, Lenaz G. On the mechanism of inhibition of NADH oxidase by ubiquinone-3. J. Bioenerg. Biomembr. 1984; 16:153–166. [PubMed: 6536673]
43. Estornell E, Fato R, Castelluccio C, Cavazzoni M, Castelli GP, Lenaz G. Saturation kinetics of coenzyme-Q in NADH and succinate oxidation in beef-heart mitochondria. FEBS Lett. 1992; 311:107–109.
44. Norling B, Glazek E, Nelson BD, Ernster L. Studies with ubiquinone-depleted submitochondrial particles - Quantitative incorporation of small amounts of ubiquinone and its effects on NAHD and succinate oxidase activities. Eur. J. Biochem. 1974; 47:475–482. [PubMed: 4154843]
45. Roche Y, Peretti P, Bernard S. DSC and Raman studies of the side chain length effect of ubiquinones on the thermotropic phase behavior of liposomes. Thermochim. Acta. 2006; 447:81–88.
46. Roche Y, Peretti P, Bernard S. Influence of the chain length of ubiquinones on their interaction with DPPC in mixed monolayers. Biochim. Biophys. Acta-Biomembr. 2006; 1758:468–478.
47. Welter R, Gu LQ, Yu L, Yu CA, Rumbley J, Gennis RB. Identification of the ubiquinol-binding site in the cytochrome bo_3 ubiquinol oxidase of *Escherichia coli*. J. Biol. Chem. 1994; 269:28834–28838. [PubMed: 7961841]

Europe PMC Funders Author Manuscripts

48. Giordani R, Buc J, CornishBowden A, Cardenas ML. Kinetics of membrane-bound nitrate reductase A from *Escherichia coli* with analogues of physiological electron donors - Different reaction sites for menadiol and duroquinol. Eur. J. Biochem. 1997; 250:567–577.

Europe PMC Funders Author Manuscripts

Europe PMC Funders Author Manuscripts

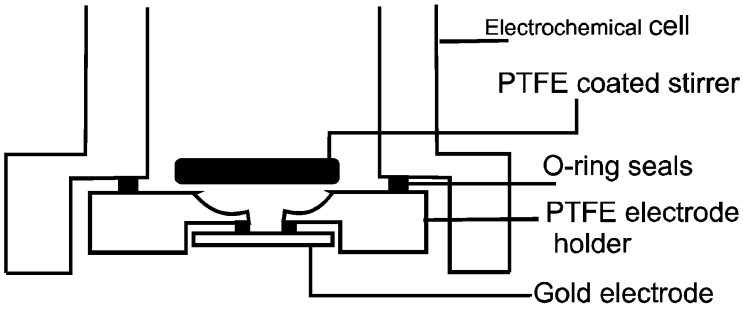

Figure 1.
Labelled diagram of the electrochemical cell with stirring.

Europe PMC Funders Author Manuscripts

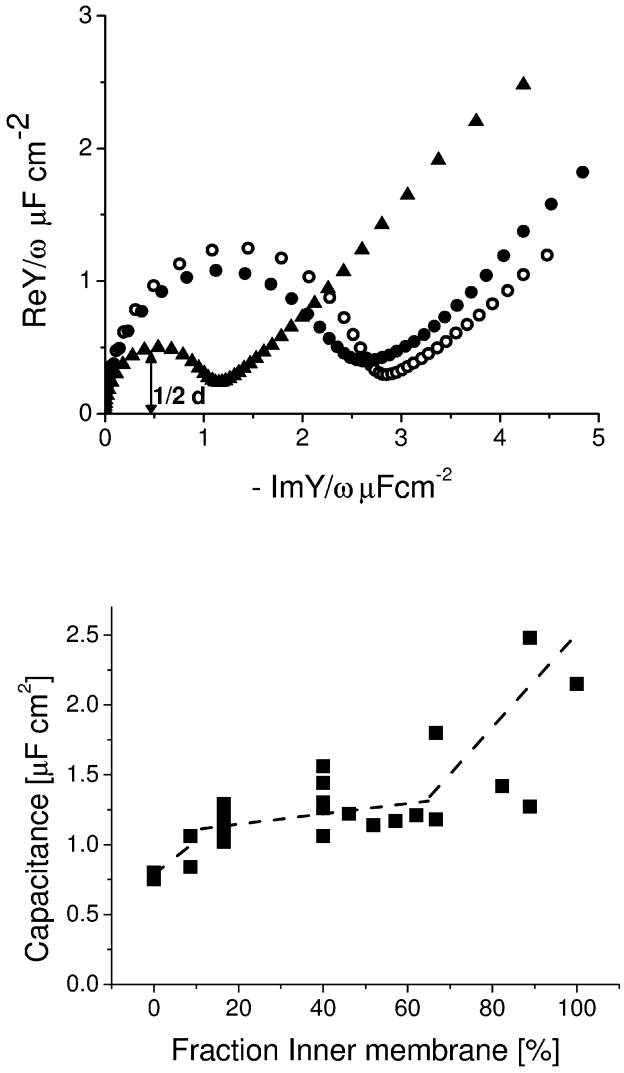

Figure 2. Cole-Cole plots of electrode characterisation

Cole-Cole plots of template-stripped electrodes modified with 60/40% (by area) of EO3-cholesteryl/6-mercaptohexanol. (open circles) without vesicles; (closed circles) inner membrane vesicles from *E. coli* and (closed triangles) mixed vesicles of 17% w/w inner membrane/lipid. The arrow indicates where the diameter of the semi-circle is to estimate the double layer capacitance. (b) Double layer capacitance of tethered native membrane surfaces at different inner membrane concentrations. The line is a guide for the eye and highlights the transition from planar bilayer to an adsorbed vesicle surface.

Europe PMC Funders Author Manuscripts

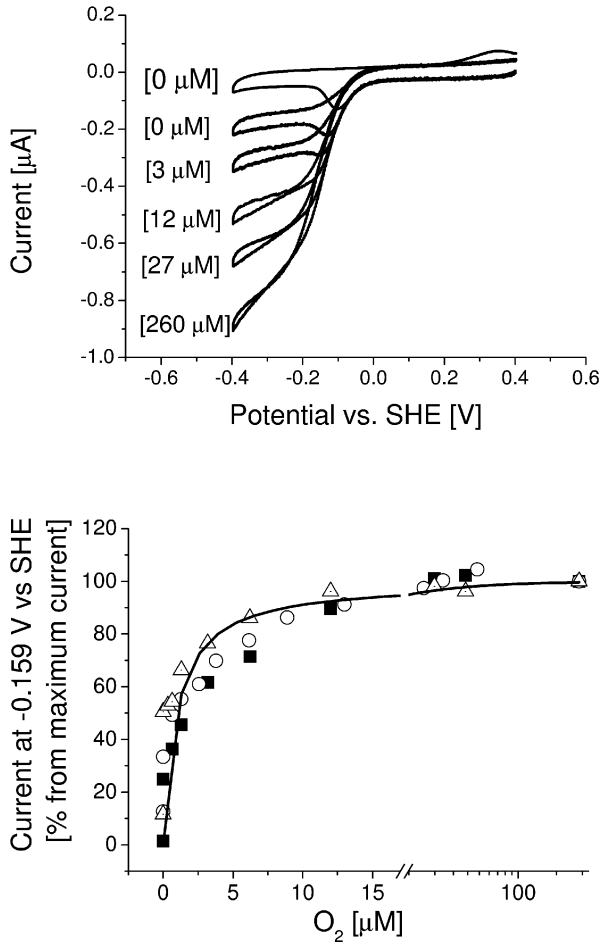

Figure 3. Activity of *cbo*$_3$ with oxygen

(a) Cyclic voltammograms at 0.01V/s showing the effect of increasing oxygen concentration on the UQ-10 pool. All CV except the first CV at 0 μM are carried out with stirring (b) Data obtained by extracting the current at −0.159 V on the reverse scan and normalising the data as % of maximum activity graph showing extracted data from three separate experiments. The solid line shows a fit to the Michaelis-Menten equation for the combined data. After the break in the x-axis, the data is plotted on a log scale for greater clarity.

Europe PMC Funders Author Manuscripts

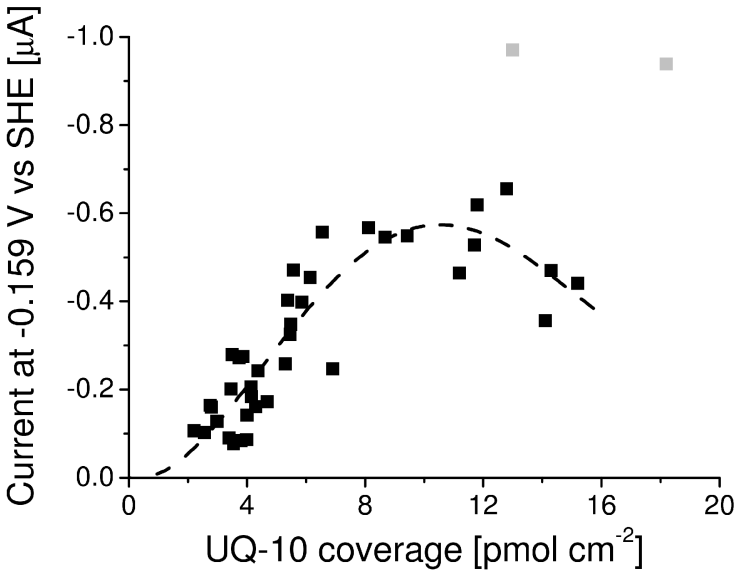

Figure 4. C*bo*$_3$ activity as a function of UQ-10 coverage

Activity was determined by taking the current at −0.159 V of the forward scan. Each data point is obtained from a separate bilayer experiment. The dotted line is guide for the eye to highlight possible cooperative behaviour as described in the discussion. The points in grey are considered to be outliers, possibly due to damaged electrode surfaces.